Article:
Gainar, Adrian, Tzeng, Mei Chun, Heinrich, Benoît et al. (2017) Incompatibility-Driven Self-Organization in Polycatenar Liquid Crystals Bearing Both Hydrocarbon and Fluorocarbon Chains. Journal of Physical Chemistry B. pp. 8817-8828. ISSN: 1520-5207

https://doi.org/10.1021/acs.jpcb.7b04490

Incompatibility-driven Self-organization in Polycatenar Liquid Crystals bearing both Hydrocarbon and Fluorocarbon Chains

Adrian Gainar[a,b], Mei-Chun Tzeng[a], Benoît Heinrich[c], Bertrand Donnio[c*] and Duncan W. Bruce[a*]

[a] *Department of Chemistry, University of York, Heslington, YORK YO10 5DD (UK)*

[b] *Current address: Department of Chemistry, Imperial College London, London, SW7 2AZ (UK)*

[c] *Institut de Physique et Chimie des Matériaux de Strasbourg (IPCMS), CNRS-Université de Strasbourg (UMR 7504), 23 rue du Loess BP 43, 67034 STRASBOURG Cedex 2, FRANCE.*

[a] **Tel: (+44) 1904 324085; E-mail: duncan.bruce@york.ac.uk*

[c] **Tel: (+33) 388107156; E-mail: bertrand.donnio@ipcms.unistra.fr*

Abstract:

The synthesis and liquid crystal properties are reported for tri- and tetracatenar mesogens in which both hydrocarbon and semiperfluorocarbon chains have been incorporated. In the tricatenar mesogens, the lamellar spacing in the smectic C phase of the all-hydrocarbon almost doubles when the isolated hydrocarbon chain is replaced by a semiperfluorinated chain on account of the localized segregation in different sublayers between the two chain types. In the tetracatenar materials, the replacement of at least one hydrocarbon chain by semiperfluorocarbon chains is sufficient to promote columnar phase formation, but when the molecule has two hydrocarbon chains at one end and two semiperfluorocarbon chains at the other, the requirement for localized phase segregation leads to the formation of a rectangular phase with very large lattice parameters. The juxtaposition of terminal chains of different nature within the same molecular structure thus leads to a reduction in mesophase symmetry and the emergence of more complex supramolecular organization.

Introduction

Fluorine plays two important general roles in liquid crystal (LC) science.[1-4] By far, the most common is as a polarizing substituent (due to its highest electronegativity of all elements, it has the propensity of attracting electron density[5,6]) that is not too dissimilar to hydrogen in size and that can modify transition temperatures,[7,8-10] affect dielectric properties, and can act as a dipolar function at chiral centers, for example in ferroelectric materials.[11,12] Its other main role is as part of a perfluoroalkyl chain where again various physico-chemical properties are affected,[13] of which most are based on the balance between fluorophilicity and hydrophobicity as in the case of medicines, cosmetics, surfactants, paints or lubricants.[14-20]

Beside the fact that the fluorine atom is slightly more voluminous than the hydrogen (mean van der Waals' radius for F = 1.47 Å; for H = 1.20 Å),[21] the C–F bond is longer than the C–H bond (typically 1.35 Å *vs* 1.09 Å)[6] so that the volume of a perfluorocarbon chain is approximately 50% more than that of a hydrocarbon chain, which can lead to steric effects when it comes to packing chains together in the same way as with dimethylsiloxane chains.[22] Furthermore, while the C–H bond is polarizable ($\Delta\chi$ = 0.35 – Pauling scale[5]), the C–F bond is not ($\Delta\chi$ = 1.43[5]). Combined with the very different polarities of the two bonds, this leads to the observation both that long hydrocarbon chains tend to be immiscible with long fluorocarbon chains and that materials bearing long fluorocarbon chains often exhibit lower viscosity than analogous materials with hydrocarbon chains.[1-4,11,13]

The immiscibility of perfluorocarbons and hydrocarbons has been exploited in, for example, catalytic chemistry where metal complexes have been bound to ligands containing so-called 'fluorous ponytails', which has facilitated catalyst separation in homogeneous situations.[23-25] Of course, if a compound contains *both* a fluorocarbon chain *and* a hydrocarbon chain, then it cannot phase separate from itself and so most properly it is referred to as an amphiphile.[26,27] This is a familiar situation in, for example, surfactant amphiphiles where the incompatibility of polar and apolar regions is solved on micellization, although it should be borne in mind that other forms of amphiphilicity are possible, for example based on shape.[28] Thus, when a self-organizing material contains two mutually immiscible parts, it needs to find an accommodation in its arrangement that takes this into account and so additional factors come into play in determining mesophase symmetry. In general terms, where a simple calamitic material contains both hydrocarbon and fluorocarbon terminal chains, lamellar phases result that are often bilayer in nature owing to the in-mesophase segregation between the different chains.[29-31] A notable exception is constituted by swallow-tailed compounds, as they form high-temperature, monolayer smectic A/C phases with undifferentiated alkyl and fluorinated layers, the differentiation appearing finally in the rectangular phases observed at lower temperature.[32,33] As a matter of fact, mesogens that are likely to form more two-dimensional mesophases (*i.e.* columnar phases) offer a potentially more intriguing prospect.[34-37]

Polycatenar mesogens, in particular, then present themselves as of interest in forming two-dimensional mesophases.[38,39] In particular, tetracatenar mesogens with 3,4-dialkoxyphenyl terminal groups are known to form a nematic (N) and lamellar (normally smectic C – SmC) phase at shorter chain lengths and a columnar phase at longer chains lengths, sometimes with a cubic phase at intermediate chain lengths.[40] This change from lamellar to columnar behavior has been explained[41,42] on the basis of the relative volume of the rigid core and of the terminal chains. Thus, as the chains occupy a greater volume either by getting longer or through increased thermal motion, there is an increasing mismatch between chain and core cross-sectional areas that leads to a break-up of a lamellar structure and the formation of what are conventionally described as columnar (Col) phases, normally with hexagonal or rectangular symmetry. We were then able to provide a thorough explanation of the organization in these columnar phases using detailed X-ray and dilatometric studies.[43] Given the depth of understanding of these polycatenar systems, they appeared the perfect choice to explore how formally amphiphilic materials might organize. The motif chosen is found in Scheme 2 and consists of a core of five phenyl rings separated by ester functions. We have reported previously on all-hydrocarbon tetracatenar derivatives of these compounds[44] and in this study, we have used synthetic approaches capable of generating unsymmetric derivatives to allow some systematic variations.

Synthesis

The unsymmetric nature of many of the target compounds led to a modular approach to the synthetic chemistry, which is described in detail in the Supplementary Information and which is summarized in Scheme 1. The semiperfluorinated alkyl chain was introduced using a tetramethylene spacer following an approach described elsewhere.[45-47] Some of the target compounds contained an unsymmetrically difunctionalized 3,4-dialkoxybenzoate unit and it is of interest to note its preparation (Scheme 1). It is also important to realize that the presence of long-chain perfluoroalkyl fragments reduces the solubility of the various compounds significantly, even when using solvents such as trifluoromethylbenzene,[48] and that this influenced aspects of the synthetic strategy. The final synthetic step to each product under consideration is shown in Scheme 2, which also shows a labelling scheme.

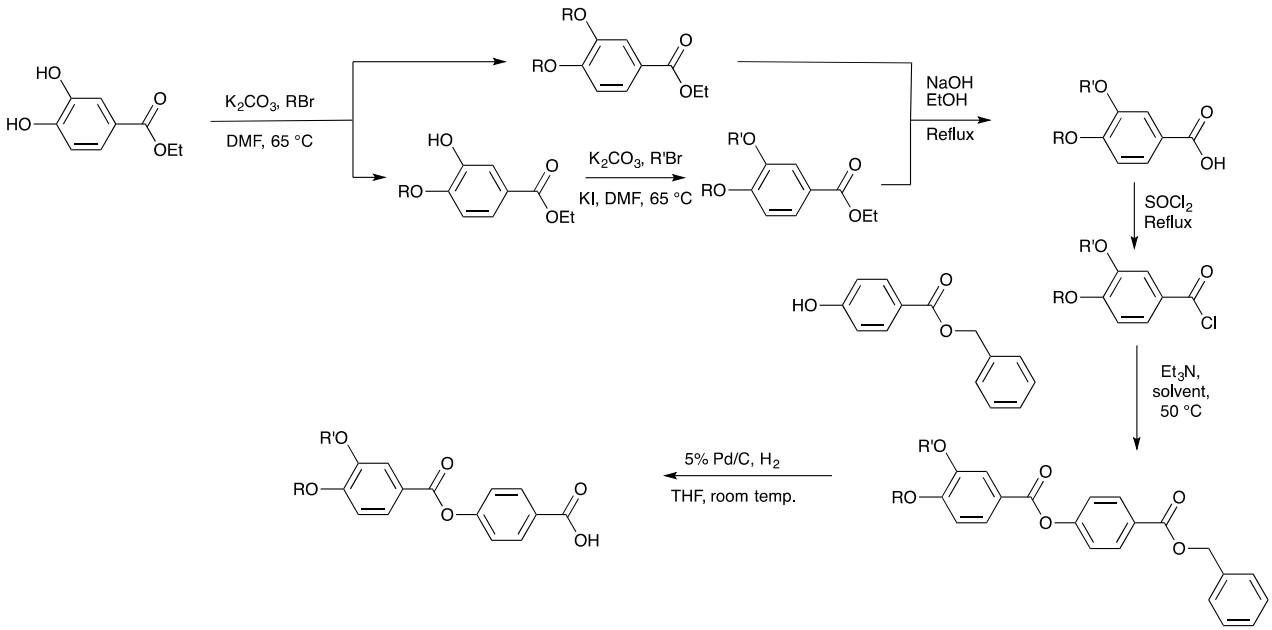

Scheme 1. Summary of the synthetic route (details in the supporting information).

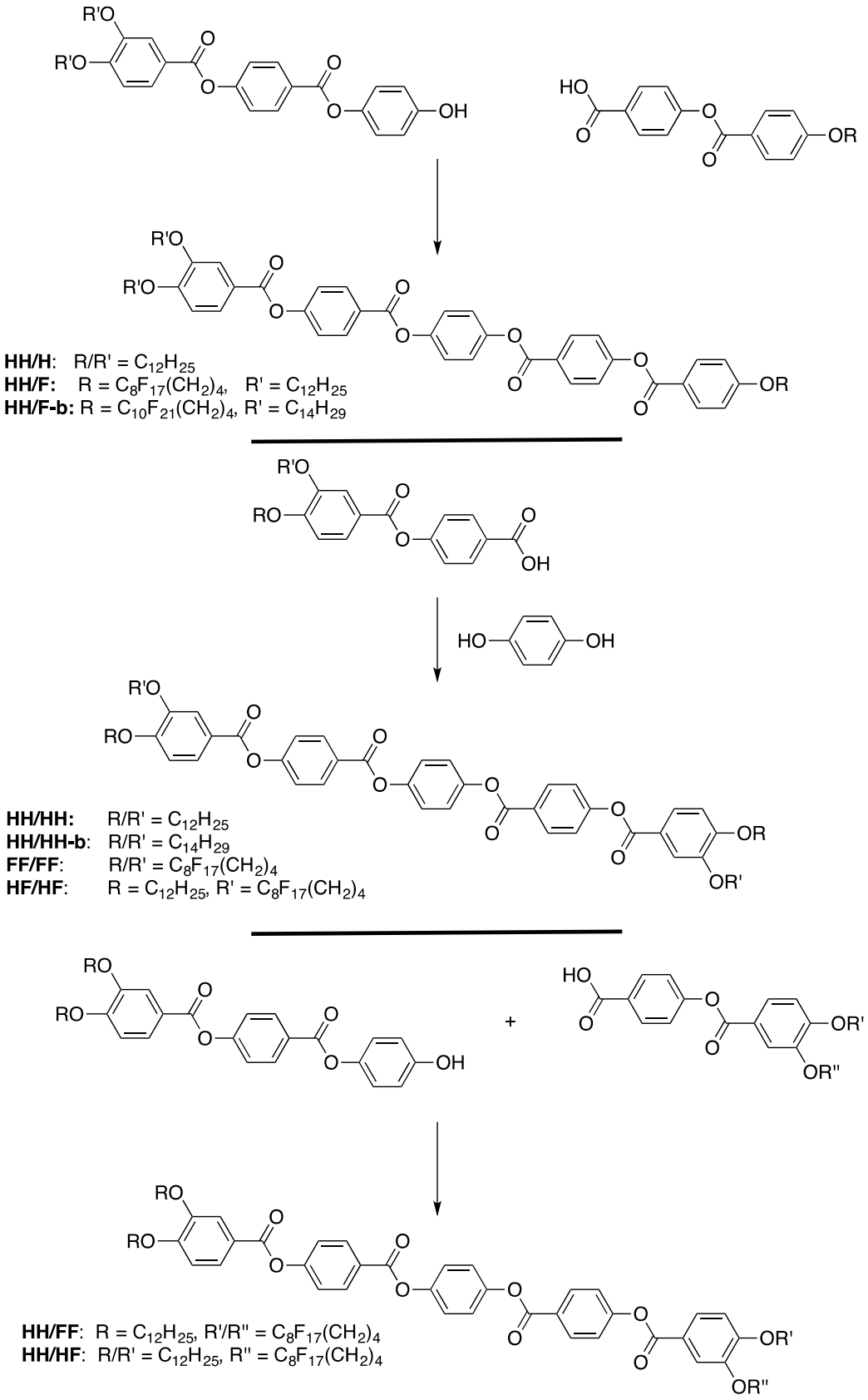

Scheme 2. Synthetic routes to the target compounds – final step. The nomenclature represents the type of chain (H = hydrocarbon, F = semiperfluorocarbon). The total number of carbon atoms in the chain is always 12 – either $C_{12}H_{25}$–(H) or $C_8F_{17}(CH_2)_4$– (F), except for two cases (indicated with **–b** at the end) where carbon chain lengths are 14 ($C_{14}H_{29}$– or $C_{10}F_{21}(CH_2)_4$–).

Mesomorphism of the Target Compounds – Optical and Structural Studies

First, it should be noted that several of the intermediate compounds have LC properties that have not been reported previously and these are collected in the Supporting Information.

The thermal behavior for the polycatenar compounds is collected in Table 1 and summarized in the phase diagram (Figure 1) with representative textures shown in Figure 2. Experimental details of how these data were obtained are found in the Supporting Information. Typical for such substitution patterns, the mesomorphism of the tricatenar compounds is dominated by the occurrence of the SmC phase, whereas for the tetracatenar homologues, both smectic and columnar mesophases are displayed.

Tricatenar compounds **HH/H** and **HH/F**[†] melt to liquid-crystalline phases giving rise to fluid textures with characteristic broken fan and Schlieren areas, recognized readily as SmC phases (Figure 2). Consistent with the anisotropy of the molecular core, the clearing point was high at *ca* 240 °C, although it was of interest to note that the melting point was as low as 132 °C. The compounds with only hydrocarbon terminal chains, *i.e.* tricatenar compound **HH/H** also showed a higher-temperature nematic phase. When the isolated hydrocarbon chain in the tricatenar compounds is replaced by a semiperfluorocarbon chain (**HH/F**), a slight enhancement of the mesomorphic range is observed whilst the melting point remains almost the same. However, the nematic phase observed in **HH/H** has totally disappeared at the expense of the SmC phase which takes over the entire mesomorphic domain.

The previously reported[49] tetracatenar compounds **HH/HH** also melt to SmC phases (Figure 1), with **HH/HH** also showing a higher-temperature nematic phase while **HH/HH-b** also exhibits a lower-temperature Col_r phase.[49] If one of the *meta*-alkyl chains of the tetracatenar compound **HH/HH** is replaced by a semiperfluorinated fragment (**HH/HF**), the crystalline phase is destabilized leading to an increase in the mesophase temperature range from less than 8°C to about 22°C (**HH/HH** *vs* **HH/HF**). This modification also affects the organization of the molecules in the mesophase, as based on the optical texture the phase is Col_h (Figure 2, *vide infra*).

The two isomeric tetracatenar mesogens with two alkyl and two semiperfluorinated chains behaved rather differently. Tetracatenar **HH/FF**, with two dodecyloxy chains at one end and two semiperfluoroalkyl chains at the other melts at a slightly higher temperature (138.6 °C) than the isomeric compound **HF/HF** (128.3 °C) into a SmC phase with a rather extended range. On further heating, a second transition leads to another mesophase that persisted for over 30 °C before clearing is observed at 208.2 °C; this second mesophase was assigned as a columnar phase (*vide infra*) on the basis of optical microscopy (Figure 2). Thus, compound **HF/HF**, which bears a semiperfluorinated chain in the two terminal *meta*-positions and hydrocarbon chains in the *para*-positions, melts at 128.3 °C to give a mesophase that persists up to 169.9

[†] Implies either semiperfluorocarbon chain length.

°C. The optical texture (Figure S3) shows clearly that the phase is columnar, and the presence of large homeotropic zones even suggests that phase symmetry is hexagonal, Col_h. It is interesting to note that the lower melting and clearing points of **HF/HF** compared to **HH/FF** suggests that the mixing of terminal (*para*) hydrocarbon and lateral (*meta*) semiperfluorocarbon chains is disruptive both to the packing in the crystal phase and the organization in the mesophase. That a *meta*-semiperfluoroalkyl chain is disruptive to crystal-phase organization is also shown when compound **HH/HF** is considered, which is a tetracatenar mesogen bearing three hydrocarbon chains and one semiperfluoroalkyl chain in a *meta*-position. Thus, while the clearing point of **HH/HH** and **HH/HF** are remarkably similar (171.9 *vs* 174.1 °C, respectively), the melting point of **HH/HF** is reduced compared to **HH/HH** (152.6 *v*s 170.2 °C, respectively). Furthermore, the mesomorphism changes from SmC and N in **HH/HH** to Col_h in **HH/HF**.

Finally, the tetracatenar compound bearing four semiperfluorinated chains (**FF/FF**) was found to exhibit a single columnar hexagonal phase over a substantial temperature range. Thus, compound **FF/FF** melts at 137.4 °C – a temperature appreciably lower than that of the analogous all-hydrocarbon analogue **HH/HH**, and clears at 259.5 °C, displaying the broadest temperature range of this series of compounds, of *ca* 122 °C.

The 1,4-phenylene-bis(4-(benzoyloxy)benzoate) structure is therefore a suitable molecular building block to design LC materials,[49] as revealed by the rich and diverse mesomorphism exhibited by both series of polycatenar mesogens. Whereas the tricatenar mesogens show a wide mesomorphic range on account of relatively low melting points a high mesophase stability, grafting of an additional aliphatic chain to give a tetracatenar materials in general leads to destabilization of the clearing point, while melting points are similar or slightly higher except for **FF/FF** with four semiperfluoroalkyl chains where the mesophase range recovers close to those of tricatenar mesogens **HH/H** and **HH/F**. As expected, moving from tricatenar systems to those that are tetracatenar leads to an evolution of the mesomorphism away from simply SmC and N to include ribbon and columnar phases, too (Figure 1). The nature of this evolution forms the basis for the following discussion.

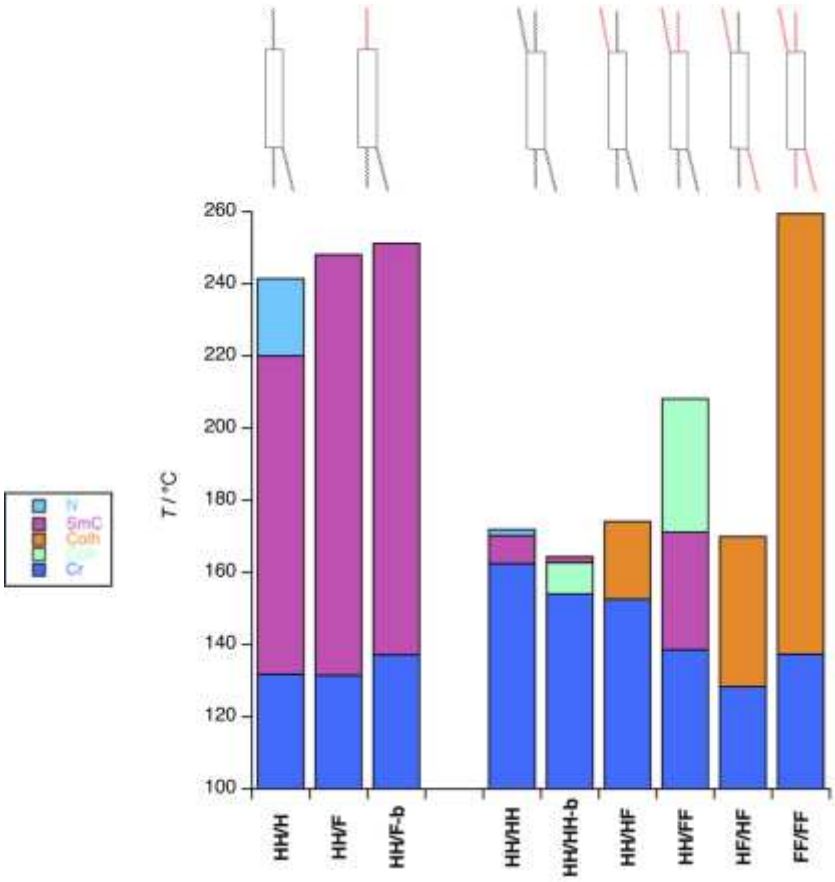

Figure 1. Bar chart showing mesophase temperatures for the compounds under study, along with a schematic molecular drawing in which hydrocarbon chains are indicated in black and fluorocarbon chains in red.

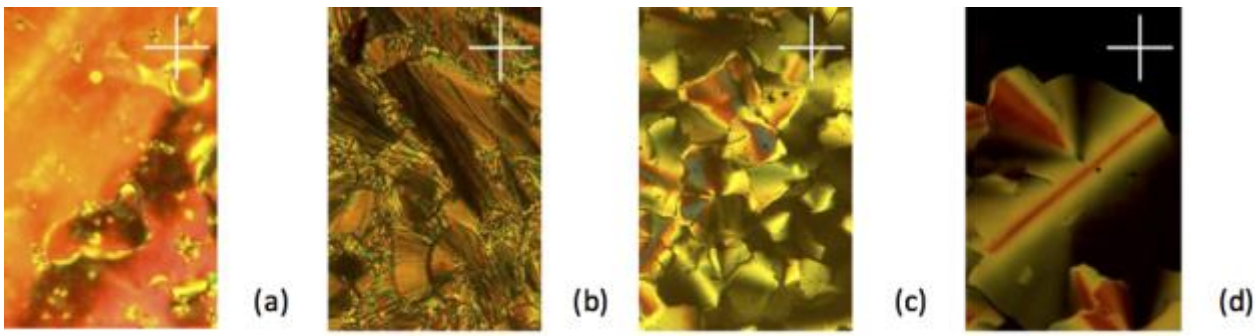

Figure 2 Representative optical micrographs (all textures obtained on cooling): (a) nematic phase of **HH/HH** at 220 °C, (b) SmC phase of **HH/F** at 160 °C, (c) Col_h phase of **FF/FF** at 160 °C, (d) Col_h phase of **HH/HF** at 150 °C.

Table 1. Thermal behavior of the compounds discussed in this study.

Compounds	Transition	*T*/°C	Δ*H*/kJ mol^{-1}
HH/H	Cr–SmC	131.8	34.5
	SmC–N	220.0	8.0
	N–Iso	241.5	1.8
HH/F	Cr–SmC	131.5	42.7
	SmC–Iso	248.1	9.0
HH/F-b	Cr–SmC	137.1	51.68
	SmC–Iso	251.2	12.73
HH/HH[a]	Cr–SmC	162.5	73.7
	SmC–N	170.2	4.7
	N–Iso	171.9	0.7
HH/HH-b[a]	Cr–Col_r	154.0	72.2
	Col_r–SmC	162.7	0.6
	SmC–Iso	164.3	8.2
FF/FF	Cr–Cr_1	117.9	–12.2
	Cr_1–Col_h	137.4	23.1
	Col_h–Iso	259.5	3.3
HH/FF	Cr–Cr_1	112.5	3.2
	Cr_1–SmC	138.6	45.9
	SmC–Col_r	171.1	2.3
	Col_r–Iso	208.2	3.6
HF/HF	Cr–Cr_1	94.5	1.93
	Cr_1–Cr_2	120.4	11.3
	Cr_2–Col_h	128.3	9.1
	Col_h–Iso	169.9	3.7
HH/HF	Cr–Cr_1	105.0	1.09
	Cr_1–Col_h	152.6	53.5
	Col_h–Iso	174.1	5.2

[a] Data from reference [49]

Cr, Cr_1, Cr_2: crystalline phases; SmC: smectic C phase; N: nematic phase; Col_r: rectangular columnar phase; Col_h: hexagonal columnar phase; Iso: isotropic liquid.

Small-Angle X-ray Scattering (SAXS)– Supramolecular Organization

The polycatenar compounds were studied by SAXS and the data and mesophase parameters are collected in Table 2. For the all-hydrocarbon compound **HH/H**, the diffraction pattern recorded at 140 °C showed only a single, low-angle reflection, which, supported by microscopy, can be attributed to the lamellar periodicity of a SmC phase of *ca* 36.85 ± 0.15 Å (001), and a broad, wide-angle signal corresponding to a

spacing of 4.6 Å, h_{max}, reflecting the superposition of the molten aliphatic chains, $\langle h_H \rangle$, and mesogenic core, $\langle h_c \rangle$ (Figure 3). For the tricatenar compounds with the semiperfluorinated chain (**HH/F** and **HH/F-b**), several orders of lamellar reflections (00*l*), up to *l* = 3 (**HH/F**) and *l* = 6 (**HH/F-b**) are observed, suggesting well-organized layers with sharp interfaces in the mesophases. The diffuse reflection at wide angle is also present but broader and slightly shifted to smaller angle (*ca* 5.0 Å) as resulting from the superposition of the reflections from the molten hydrocarbon/core $\langle h_c h_H \rangle$ and fluorocarbon $\langle h_F \rangle$ chains, whose maxima are expected at 4.76, 4.73 and 5.77 Å, respectively (Figure 3, Table 2). Indeed, the theoretical position of the scattering maximum is notably different for semiperfluorocarbon chains and hydrocarbon chains (the latter coinciding with mesogens), but contributions are not resolved and only a broad maximum is observed whose position depends on the proportion of semiperfluorocarbon chains (Figures 3 & 4).

The SAXS data for **HH/FF** at various temperatures confirm the presence of two mesophases. The lamellar nature of the lower-temperature phase was deduced from the presence of three small-angle reflections in the 1:2:3 ratio, again suggesting well-correlated layers, along with the broad halo, h_{max}, at wide angles (Figure 2). The obvious feature when comparing **HH/H** with the other smectogens **HH/F** and **HH/FF**, is the almost exact doubling of the lamellar periodicity in **HH/F** (76.4 Å), **HH/F-b** (82.3 Å) and **HH/FF** (76 Å), suggesting a bilayer organization in these last three. The distinctly amphiphilic nature of **HH/F** and **HH/FF** likely imposes this organization owing to the mutual immiscibility of the terminal hydrocarbon and fluorocarbon chains.

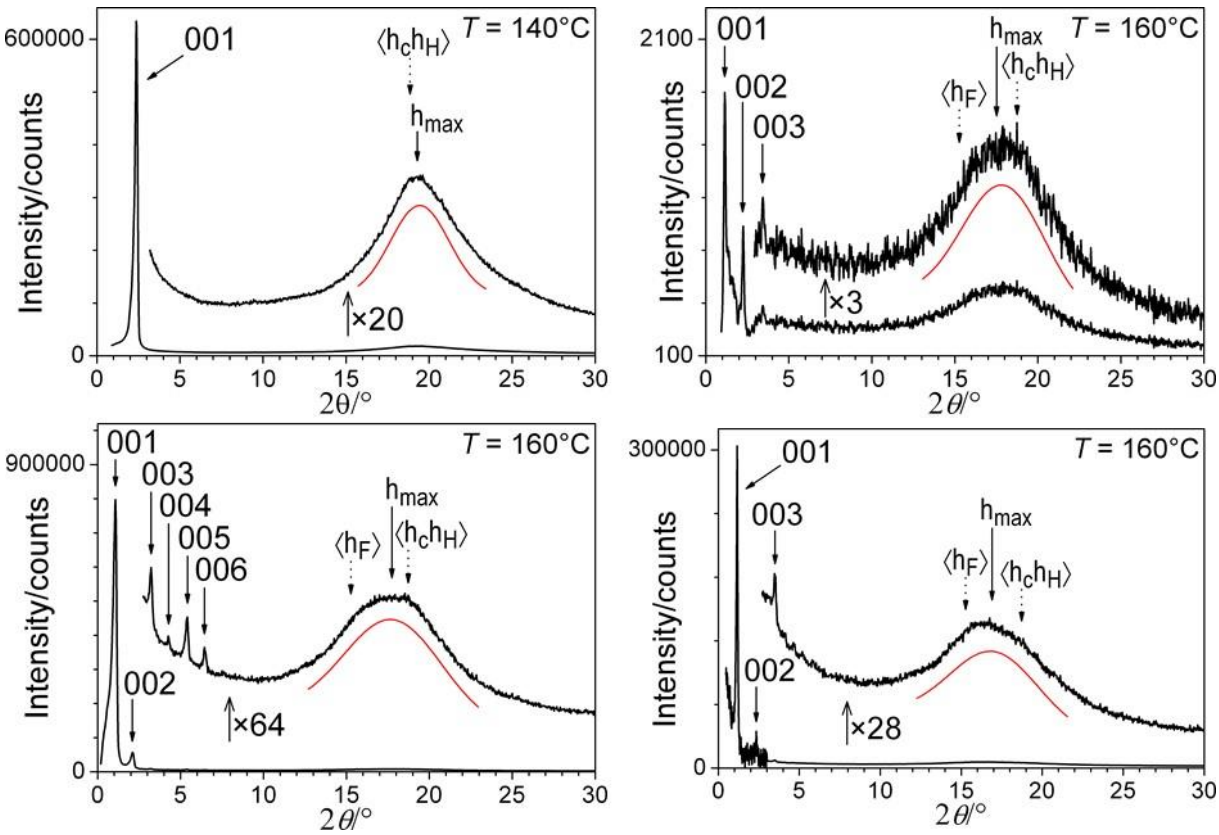

Figure 3. SAXS patterns of **HH/H** (SmC; top left), **HH/F** (SmC; top right), **HH/F-b** (SmC; bottom left), **HH/FF** (SmC; bottom right); the small-angle part of **HH/FF** (<3°) comes from image plate scan and the wide-angle part, from acquisition with gas-filled detector.

SAXS investigations of the other tetracatenar mesogens also confirm their LC nature (Figure 3). They are all characterized by a strong diffuse wide-angle scattering with a maximum of diffusion at *ca* 5.1-5.5 Å (h_{max}), which corresponds, as mentioned already to the superposition of the diffuse signals $\langle h_H \rangle$, $\langle h_F \rangle$ and $\langle h_c \rangle$.

The SAXS pattern of **FF/FF** at 180 °C confirms the hexagonal nature of the mesophase, revealing small-angle reflections with relative spacings 1:√3:√7 and the lattice parameter a = 53.1 Å. In this case, the diffraction pattern shows rather low-intensity reflections (Figure 3) on account of there being little electronic contrast between the unsaturated rings in the core of the molecule and the perfluorocarbon fragments at the extremities, which are only separated by a very small volume fraction of aliphatic spacer (of lower electronic density). The lattice parameter is almost constant across the temperature range.

For the higher-temperature phase of **HH/FF** (*vide supra*), there are enough reflections to enable identification of the phase symmetry and the assignment of the two observed reflections as (20)/(11), and (12) is in agreement with a non-centered, rectangular lattice (*p*2*gg*). The lack of centrosymmetry is ascertained by the presence of the (12) reflection (this excludes centering on the basis of the extinction rule: $h + k = 2n + 1$). It is likely that this phase arises from a modulation of the underlying lamellar phase to

give a superlattice with a = 160.3 Å and b = 92.5 Å (a/b = √3). The isomeric compound, **HF/HF**, showed only a single, small-angle reflection, which, supported by microscopy, confirms the presence of the Col_h mesophase. However, the fundamental reflection shows reduced intensity, once more due to the low-contrast between fluorinated domains and ribbons of aggregated aromatic cores. In addition, the localized separation between fluorinated and hydrogenated domains leads to a loosely correlated, short-range periodicity D, at *ca* 19 Å (ξ = 25 Å). Finally, the SAXS pattern of **HH/HF** is almost identical to that of **HF/HF**, which, again combined with microscopy (Figure 2) confirms the Col_h structure of the mesophase and loosely correlated domain structure is again seen in a mid-angle reflection (D = 19 Å; ξ = 25 Å).

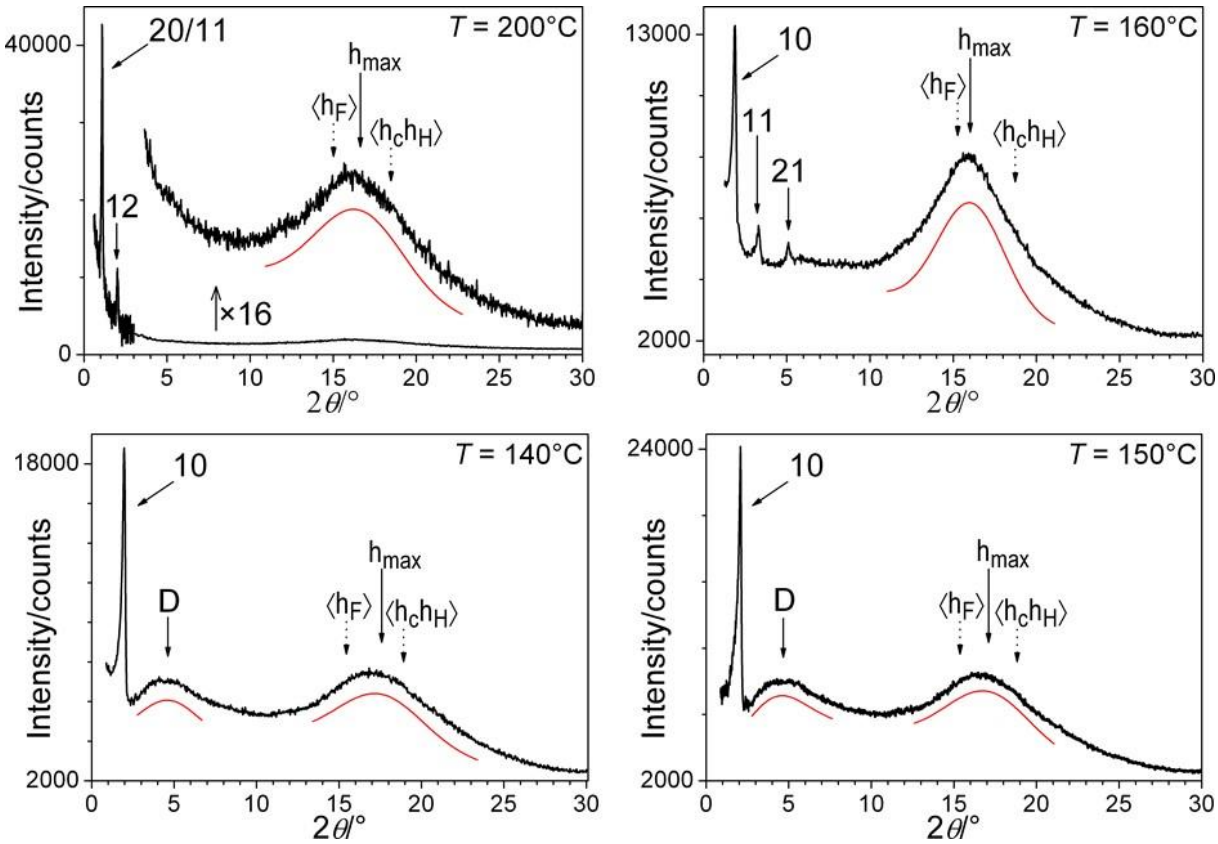

Figure 4. SAXS patterns of **HH/FF** (Col_r; top left), **FF/FF** (Col_h; top right), **HF/HF** (Col_h; bottom left), **HH/HF** (Col_h; bottom right); the small-angle part of **HH/FF** (<3°) and **HH/HF** (<2.6°) comes from image plate scan and the wide-angle part, from acquisition with gas-filled detector.

Table 2. X-ray and structural data for the mesophases of the polycatenar mesogens

d_{meas}/Å	*hkl*	Intensity	d_{calc}/Å	Parameters
			HH/H	
36.85	001	VS (sh)	36.85	T = 140 °C, SmC
4.6	-	VS (br)	h_{max}	d = 36.85 Å (N_L = 1)
				V_{mol} = 1870 Å^3 (ρ= 0.99)
				A_{mol} = 50.7 Å^2
				a_c, σ_c = 50.7, 23.5 Å^2; ψ_c = 62°
				a_H, σ_H = 33.8, 23.1 Å^2; q_H = 1.46
				$\langle h_c \rangle$, $\langle h_H \rangle$ = 4.73, 4.70 Å

			HH/F	
76.0	001	VS (sh)	76.43	T = 160 °C, SmC
38.37	002	S (sh)	38.21	d = 76.4 Å (N_L = 2)
25.5	003	M (sh)	25.47	V_{mol} = 2060 Å^3 (ρ = 1.14)
5.0	-	VS (br)	h_{max}	A_{mol} = 27.0 Å^2
				a_c, σ_c = 54.0, 23.8 Å^2; ψ_c = 64°
				a_H, σ_H = 27.0, 23.5 Å^2; q_H = 1.15
				a_F, σ_F = 54.0, 34.9 Å^2; q_F = 1.55
				$\langle h_c \rangle$, $\langle h_H \rangle$, $\langle h_F \rangle$ = 4.76, 4.73, 5.77 Å
			HH/F-b	
81.9	001	VS (sh)	82.30	T = 160 °C, SmC
41.38	002	S (sh)	41.15	d = 82.3 Å (N_L = 2)
27.46	003	M (sh)	27.43	V_{mol} = 2270 Å^3 (ρ = 1.15)
20.58	004	VW (sh)	20.57	A_{mol} = 27.6 Å^2
16.45	005	M (sh)	16.46	a_c, σ_c = 55.2, 23.8 Å^2; ψ_c = 65°
13.7	006	W (sh)	13.72	a_H, σ_H = 27.6, 23.5 Å^2; q_H = 1.18
5.0	–	VS (br)	h_{max}	a_F, σ_F = 55.2, 34.9 Å^2; q_F = 1.58
				$\langle h_c \rangle$, $\langle h_H \rangle$, $\langle h_F \rangle$ = 4.76, 4.73, 5.77 Å
			FF/FF	
46.26	10	M (sh)	45.96	T = 160 °C, Col$_h$
26.73	11	M (sh)	26.53	a = 53.1 Å; A = 2440 Å^2 (Z = 1)
17.33	21	M (sh)	17.37	V_{mol} = 2940 Å^3 (ρ = 1.42)
5.5	-	VS (br)	h_{max}	S = 2440 Å^2; h_{mol} = 1.21 Å; N_c = 4.6
				$a_{cyl1,H}$, σ_H = 26.4, 23.5 Å^2; q_H = 1.13
				$a_{cyl2,F}$, σ_F = 33.9, 34.9 Å^2; q_F = 0.97
				$\langle h_c \rangle$, $\langle h_H \rangle$, $\langle h_F \rangle$ = 4.76, 4.73, 5.77 Å
			HH/FF	
76.0	001	VS (sh)	75.90	T = 160 °C, SmC
37.95	002	S (sh)	37.95	d = 75.9 Å (N_L = 2)
25.3	003	M (sh)	25.30	V_{mol} = 2600 Å^3 (ρ = 1.22)
5.2	–	VS (br)	h_{max}	A_{mol} = 34.3 Å^2
				a_c, σ_c = 68.5, 23.8 Å^2; ψ_c = 70°
				a_H, σ_H = 34.3, 23.5 Å^2; q_H = 1.46
				a_F, σ_F = 34.3, 34.9 Å^2; q_F = 0.98
				$\langle h_c \rangle$, $\langle h_H \rangle$, $\langle h_F \rangle$ = 4.76, 4.73, 5.77 Å
80.3	11/20	VS (sh)	80.15	T = 200 °C, Col$_r$
44.4	12	S (br)	44.46	a, b = 160.3, 92.5 Å; A = 14840 Å^2 (Z = 6)
5.4	–		h_{max}	V_{mol} = 2680 Å^3 (ρ = 1.18)
				S = 2473 Å^2; h_{mol} = 1.08 Å; N_c = 5.0
				$a_{cyl1,H}$, σ_H = 25.2, 24.1 Å^2; q_H = 1.04
				$a_{lay,F}$, σ_F = 33.4, 35.9 Å^2; q_F = 0.93
				$\langle h_c \rangle$, $\langle h_H \rangle$, $\langle h_F \rangle$ = 4.82, 4.79, 5.85 Å
			HF/HF	
44.25	10	VS (sh)	44.25	T = 140 °C, Col$_h$
19	–	S (ξ = 25 Å)	D	a = 51.1 Å; A = 2261 Å^2 (Z = 1)
5.1	–	VS (br)	h_{max}	V_{mol} = 2570 Å^3 (ρ = 1.23)
				S = 2261 Å^2; h_{mol} = 1.14 Å; N_c = 4.5
				$a_{cyl1,H}$, σ_H = 25.6, 23.1 Å^2; q_H = 1.11
				$a_{cyl2,H/F}$, $\sigma_{H/F}$ = 32.8, 28.8 Å^2; $q_{H/F}$ = 1.14
				$\langle h_c \rangle$, $\langle h_H \rangle$, $\langle h_F \rangle$ = 4.73, 4.70, 5.73 Å
			HH/HF	
42.33	10	S (sh)	42.33	T = 150 °C, Col$_h$

19	–	S (ξ = 25 Å)	D	a = 48.9 Å; A = 2069 Å^2 (Z = 1)
5.2	–	VS (br)	h_{max}	V_{mol} = 2420 Å^3 (ρ = 1.10)
				S = 2069 Å^2; h_{mol} = 1.17 Å; N_c = 4.4
				$a_{cyl1,H}$, σ_H = 26.0, 23.3 Å^2; q_H = 1.12
				$a_{cyl2,H/F}$, $\sigma_{H/F}$ = 33.3, 25.8 Å^2; $q_{H/F}$ = 1.29
				$\langle h_C \rangle$, $\langle h_H \rangle$, $\langle h_F \rangle$ = 4.74, 4.71, 5.75 Å

d_{meas} and d_{calc} are the measured and calculated diffraction spacings [d_{calc} is deduced from the following mathematical expressions: $d_{00l} = 1/N_l(\sum d_{00l} \times l)$, where N_l is the number of 00l reflections observed for the lamellar phases; $a = 2(\sum d_{hk} \times (h^2+k^2+hk)^{½}/N_{hk}V3$, where N_{hk} is the number of hk reflections observed for the Col$_h$ phase, $1/d_{hk} = \sqrt{(h^2/a^2+k^2/b^2)}$ for the Col$_r$]. hkl are the Miller indexations of the reflections corresponding to the lamellar (00l) and columnar (hk) phases, respectively. Intensity of the sharp reflections: VS – very strong, S – strong, M – medium, VW – very weak); sh and br stand for sharp and broad reflection; h_{max} is the position of the wide-angle scattering maximum, which is the superposition of the contributions from molten hydrocarbon <h_H>, core <h_c> and fluorocarbon <h_F> layers 〉; D is a short-range correlated periodicity (ξ: correlation length from Scherrer equation). V_{mol}, σ_C, σ_H, σ_F: calculated molecular volume (ρ corresponding density in g cm^{-3}) and natural cross-sections, obtained from reference dilatometric measurements;[26,41] $\langle h_c \rangle$, $\langle h_H \rangle$, $\langle h_F \rangle$: average lateral distance between molten segments, calculated from equation: $\langle h_i \rangle = 0.9763\sigma^{0.5}$, where i = C, H and F;[50] SmC phase. d, N_L: periodicity of SmC phase and number of molecular layers per lamella; $A_{mol} = V_{mol}/d$: molecular area; $a_C = A_{mol}N_L/n_C$, $a_H = A_{mol}N_L/n_H$, $a_F = A_{mol}N_L/n_F$: layer areas covered by single mesogen, alkyl chain and fluorinated chain, with n_F, n_C and n_H being the number of C, F or H segments per sub-layer (for **HH/H**, **HH/F**, **HH/F-b**, **HH/FF**: n_c = 1, 1, 1, 1; n_H = 3/2, 2, 2, 2; n_F = 0, 1, 1, 2); $\psi_c = \arccos(\sigma_c/a_c)$: average polar tilt angle of mesogenic cores inside the lamellae; $q_H = a_H/\sigma_H$, $q_F = a_F/\sigma_F$: chain packing ratios (q_i = 1 for flat layers and fully stretched chains). Col$_r$ and Col$_h$ phases. a, b: lattice parameters (a, b in the Col$_r$ phase, $a = b$ in the Col$_h$ phases), A, Z: lattice area and number of columns of mesogenic cores per lattice; $S = A/Z$: area per column, $h_{mol} = V_{mol}/S$: molecular slice thickness (*i.e.* the height of the column segment containing a single molecule), $N_c = h_{max}/h_{mol}$: number of aggregated molecules per columnar section, for intermolecular distance h_{max}. $a_{cyl1,H} = \pi(4/\pi x_c S)^{0.5} h_{mol}/n_{H/F}$: area per alkyl spacer at the interface between columnar cores and internal aliphatic shell assuming cylindrical column shape, x_c being the volume fraction of the mesogenic cores (**HH/FF**, **FF/FF**, **HH/HF**, **HF/HF**: x_c = 0.2774, 0.2507, 0.3035, 0.2851), $q_H = a_{cyl1,H}/\sigma_H$: chain packing ratio of the alkyl spacers near the interface.[51,52] $a_{lay,F} = bh_{mol}/(Z/N_{lay,F})$: layer area covered by a single fluorinated chain in the Col$_r$ phase of **HH/FF**, $N_{lay,F}$ being the number of fluorinated layers per lattice ($N_{lay,F}$ = 2), $q_F = a_{lay,F}/\sigma_F$: chain packing ratio of the fluorinated chains. $a_{cyl2,H/F} = \pi(4/\pi x_{CH} S)^{0.5} h_{mol}/n_{H/F}$: area per terminal chain at the boundary between the internal aliphatic shell and the external F shell (**FF/FF**) or mixed F/H (**HF/HF**, **HH/HF**) shell in the Col$_h$ phases, the boundary shape being assumed cylindrical, and x_{CH} representing the total volume fraction of mesogenic cores, alkyl spacers of F tails and segments of H tails of same length as spacers (**FF/FF**, **HH/HF**, **HF/HF**: x_{CH} = 0.4128, 0.4990 0.4681). $\sigma_{H/F} = (n_H\sigma_H + n_F\sigma_F)/(n_H+n_F)$: average cross section of the terminal chains, n_H and n_F being the number of H and F tails in a molecule. $q_{H/F} = a_{cyl2,H/F}/\sigma_{H/F}$: chain packing ratio of terminal chains near the boundary with the internal shell.

Discussion

Bearing hydrocarbon and fluorinated chains within the same molecular structure, it was anticipated that these mesogens may demonstrate the effects of hydrocarbon/fluorocarbon immiscibility within the mesomorphism of single compounds.[53-55] Smectic phases (*i.e.* lamellar phases with a planar interface) are found primarily for classical calamitic materials, with single alkyl chains at both ends of the rod-like mesogenic unit as the natural cross sections of chains (σ_H) and mesogen core (σ_c) are very similar. However, where there is a significant mismatch between the cross sections of the core and the terminal chains as found in polycatenar compounds, then smectic phase formation can become disfavored, but this mismatch can be offset to some degree if there is significant tilting of the molecular core. This is indeed what occurs with tetracatenar mesogens and SmC phases with high tilt angles appear. However, such

large tilts affect the lateral arrangement of the mesogen sublayers to accommodate the spatial requirements of the chains[56] and above a certain point, the mesogen sublayers will eventually split into ribbons that define phases most commonly described as columnar.[57]

Thus, in tricatenar mesogen **HH/H**, the presence of two terminal chains at one end causes tilting to form a SmC phase and the difference in volume at the two ends may well be accounted for by some interdigitation or chain folding (the spacing is much shorter than the molecular length). Introducing a single, terminal fluorocarbon chain (**HH/F**) alleviates the difference in volume since the cross-sectional area of fluorocarbon chains is 50% greater than that of their hydrocarbon equivalents (Table 2).

The greater volume of the semiperfluorinated chain also modifies the lateral packing. Thus, the overall space requirement of the terminal chains of **HH/F** (single semiperfluorocarbon chain) can be regarded as intermediate between those of **HH/H** (single hydrocarbon chain) and **HH/HH** (two hydrocarbon chains), and so shows a SmC phase. However, the nematic phase vanishes (common where there are fluorocarbon chains) and the smectic range extends slightly with a slightly higher clearing point compared to the all-hydrocarbon compound **HH/H**, revealing the improved confinement into layers in the presence of fluorinated tails.

SAXS data are consistent with the assignment of the SmC phase, as patterns show sharp, small-angle reflections from the lamellar periodicity as well as a broad, wide-angle scattering signal from liquid-like lateral distances inside the layers. The lamellar periodicity trivially corresponds to a single mesogen/chain alternation in **HH/H** if a tilt angle >60° is assumed, but the periodicity doubles in the presence of the semiperfluorinated chain, due to the requirement for formation of a bilayer structure owing to the mutual immiscibility of the two chain types (Figure 5). The numerous higher-order reflections visible for **HH/F** suggest well-defined layers with sharp interfaces between sublayers. Looking now to the other structural data for **HH/F**, the ratio of the statistical area effectively covered by chains and of their overall minimum cross-section, *i.e.* the chain packing ratio, q_H, stays quite close to unity ($q_H \approx 1.15$, Table 2), whereas the larger value for **HH/H** ($q_H \approx 1.46$), combined with the absence of higher-order reflections, indicates a SmC phase with less well defined layers analogous to the situation found in the SmC phase of more conventional calamitic mesogens, although with the possibility of layer undulations. As detailed previously for related polycatenar systems,[44] such undulations represent a low-energy compensation that offsets the cross-sectional mismatch allowing the chain volume to be spread out laterally. The change in the molecular organization between **HH/H** and **HH/F** suggests that this mechanism is suppressed most likely due to the segregation of the single semiperfluorocarbon chain ($q_F \approx 1.55$), which limits the lateral expansion of the chain volume. Consistently, the doubling of the semiperfluorocarbon chains in **HH/FF** imposes larger q_H values (≈1.46) and re-activates the lateral spreading and undulation mechanism, with the result that higher-order reflections almost vanish again.

Turning now to the tetracatenar materials, it is instructive to consider the effect of adding semiperfluorocarbon chains. Thus, addition of one such chain in the 3-position (**HH/HF**) leads to the observation of a Col_h phase, which is readily understood simply in terms of the increase in terminal chain volume. With this observation in hand, then it would be expected that the addition of a second chain to give a 3,3'-disemiperfluorocarbon analogue (**HF/HF**) also leads to observation of a Col_h phase. Likewise then, compound **FF/FF** with four semiperfluorocarbon chains also shows a Col_h phase. In the case of **FF/FF**, it is possible to say something about the organization, which consists of ribbons of mesogens surrounded by a thin shell of aliphatic spacer (tetramethylene spacer) and then a fluorinated peripheral continuum; the similarity in scattering length density between the mesogen core and the perfluorinated continuum explains the weakness of the first-order reflection. However, the presence of quite intense (11) and (21) reflections is also of note, since tetracatenar systems with only hydrocarbon chains often give rise to patterns without higher-order reflections.[44] This feature implies well-defined and quite sharp interfaces consistent with the chain packing ratio, q_F that is close to unity revealing the close-packed nature of the fluorocarbon chains. The similarity in the hexagonal lattice parameter between **FF/FF**, **HF/HF** and **HH/HF** (53.1, 51.1 and 48.9 Å, respectively) shows that in the last two, the incompatibility of the hydrocarbon and fluorocarbon chains is accommodated readily to allow formation of the hexagonal phase. That said, the presence of the broad, mid-angle reflection, *D* with a periodicity of 19 Å shows evidence for localized, periodic 'islands' of fluorocarbon that separate from the hydrocarbon chains reflecting their mutual incompatibility. These 'islands' moreover likely interfere with the cohesion between neighboring columns,[58] with larger islands causing greater interference as evidenced by the lower transition temperatures observed for **HF/HF** with respect to **HH/HF**. This may account for differences in mesophase stability.

As discussed elsewhere,[41,44] layer undulations can be seen as a prelude to the breaking up of the layered structure into ribbon-like phases, which are normally labeled as columnar of one sort or another and this is seen in the thermal behavior of **HH/FF** where the SmC phase gives way to a higher-temperature phase at 170 °C with a pseudo-focal conic optical texture (Figure S6). By comparison with the wide literature of the subject, in polycatenar mesogens this higher-temperature phase would be expected to be Col_h, but **HH/FF** bears two hydrocarbon chains at one end and two semiperfluorocarbon chains at the other, so that any organization beyond the SmC phase would need to accommodate its amphiphilic nature. In the SmC phase, the SAXS data again show the sharp interfaces (four orders of lamellar reflection), prevalent with terminal fluorocarbon chains, while in the higher-temperature phase, the loss of lamellar order is evidenced by a shift toward small-angles of the first-order periodicity and the appearance of a unique, higher-order reflection, some other smaller-angle reflections with the wide-angle reflection remained unchanged. These reflections were tentatively indexed in a primitive rectangular lattice with $a/b = \sqrt{3}$ and with large lattice parameters (a = 160.3 Å, b = 92.5 Å).[41,44,59] The formation of this rectangular lattice, which will for now be termed Col_r, then reflects the fact that the terminal chain volumes are too large to continue to accommodate a lamellar (SmC) phase, yet the amphiphilicity of the molecule means that it is unable to organize into a phase with hexagonal symmetry. Thus, the phase symmetry is reduced and, in

order to accommodate the incompatibility of the two chain types, a large, rectangular lattice results. The lattice will then consist of the periodic alternation of strata of hydrocarbon and fluorocarbon continuums, the cores (columns) being found contiguous with the hydrocarbon chain continuum and the periodicity of these strata (recognizing the formation of a double-layer structure) coincides with the first-order reflection inferring that the organization has a lamellar element (Figure 5). As such, while we persist with the Col_r nomenclature for the purposes of this discussion and for comparability with the wider literature, it is perhaps inappropriate to refer to the phase as columnar, rather falling back on an analogy with ribbon-like phases such as the SmÃ and B1 phases, both of which also have rectangular symmetry,[60] proposed in good faith, whose use perpetuates in the literature, there is no regular, repeating 'slab' containing two or more molecules. Indeed, the data show that the cores of these molecules are absolutely not perpendicular to the 'column' direction and that the notion of the number of molecules, *Z*, in a repeat is little more than a calculation of a notional repeat distance based on hydrocarbon separation and column dimensions. As such, any value of *Z* obtained refers to an equivalent molecular volume rather than to whole, discrete molecules. As such then, the so-called columnar phases of polycatenar molecules are more properly considered as ribbon phases. Making such a distinction does not in any way invalidate the earlier assumption concerning phases not being defined by the type of molecule of which they are composed for, as pointed out above, the Col_r, SmÃ and B1 phases are all in effect rectangular ribbon phases yet each arises from a different molecular type. The larger question is then how one might distinguish between the Col_h phase of discs and of polycatenar materials. This matter requires greater reflection and a more wide-ranging discussion and will be reported elsewhere in due course.

A possible organizational model consistent with the structural information available for **HH/FF** is then proposed (Figure 5) and in considering it and the following description, it is important to stress that it is a static 2-D projection of a dynamic 3-D arrangement. Thus, the figure shows an effectively continuous ribbon in red representing the molecular cores surrounded by alkyl chains (grey). The alkyl area arises from the tetramethylene spacer at one end of the molecule and the alkyl chain at the other, and this is reflected in the differing thicknesses represented in the figure. The blue continuum is then the fluorocarbon fragment and the larger apparent volume reflects the greater volume of fluorocarbon over hydrocarbon chain as discussed earlier. The figure shows that the various interfaces are not planar (rather they undulate), which supports both the fact that the phase is formed above the SmC phase (volume mismatches and fluctuations drive the phase out of a simple lamellar arrangement consistent with all of the earlier published work on tetracatenar mesogens referenced throughout the paper) and also that $q_F < 0$. As argued previously, it can be the case that volume mismatches are accommodated by chains escaping out of the notional ribbon plane (not easily represented in a 2-D figure) and of course it is important to recall that the perfluoroalkyl segments of the chains are attached *via* a very flexible tetramethylene linker. Thus, the static, 2-D projection in the figure shows differing apparent thicknesses of the different chain types and, where these are thinner, then it can be assumed that they escape into the third dimension.

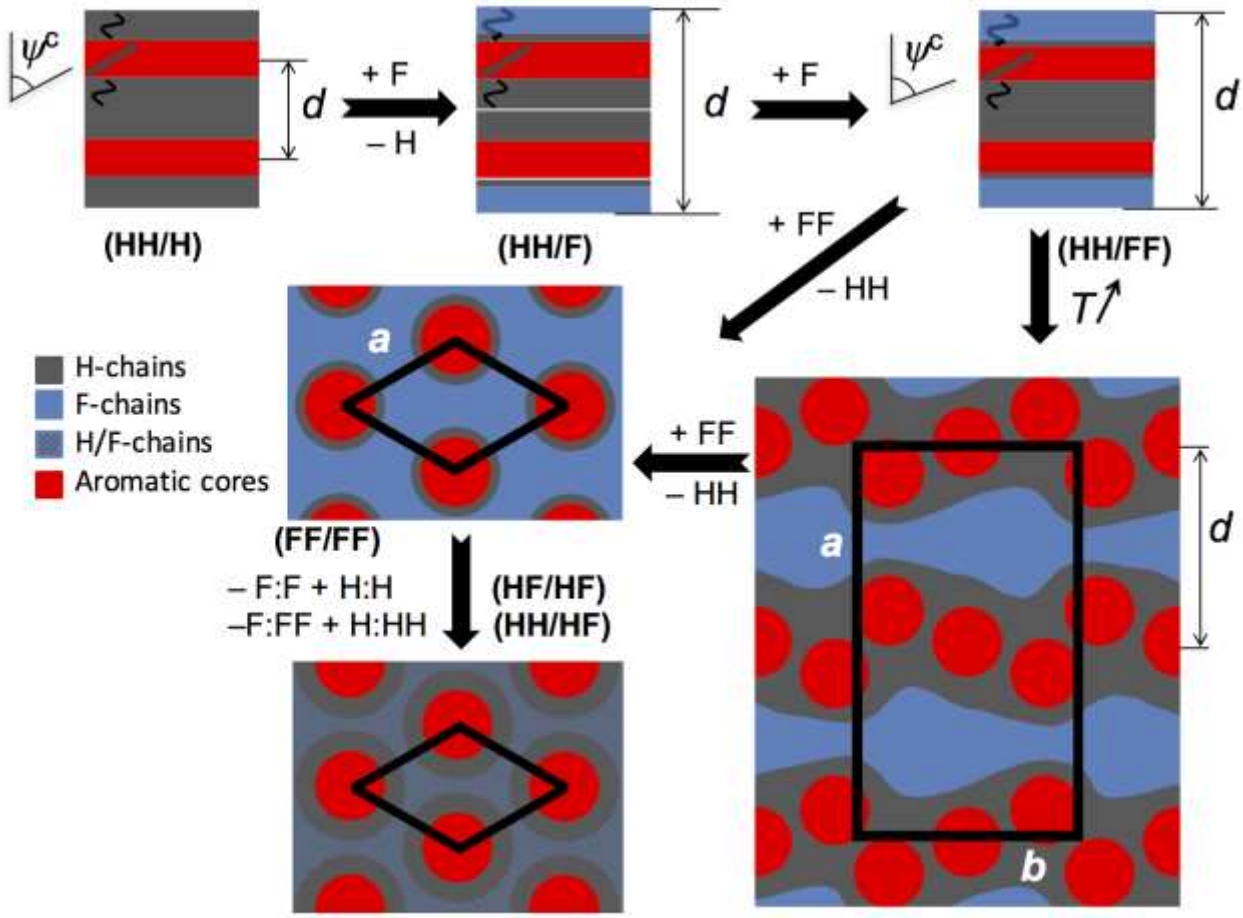

Figure 5. Schematic representation of the evolution of the molecular packing and the supramolecular organization in the mesophases as a function of the number, nature and position of hydrocarbon and semiperfluorocarbon chains within the molecular structures of the series of polycatenar compounds **HH/H** to **HH/HF**; SmC phases (**HH/H**, **HH/F/HH/F-b**, **HH/FF**): mesogens are represented by grey rods, alkyl chains by black strips and fluoroalkyl chains by blue strips; in the Col_r phase (**HH/FF**): the black frame is the rectangular lattice and *d*, the spacing of column rows; the red circles inside grey domains schematize the cross-sections of the columns formed by a break-up of the layers of mesogens and surrounded by aliphatic spacers and tails (H), while the blue strips are regions of fluorinated chains (F). Note that the ribbons of mesogens are relatively free to adopt any orientation, so they are averaged to circular columns in the mean lattice and nothing is implied concerning the organization of the mesogens within these columns. In the Col_h phases (**FF/FF, HF/HF**, **HH/HF**), the black lozenge illustrates the hexagonal lattice; columns and aliphatic periphery are schematized by red circles and grey rings, respectively, and the peripheral continuum of F chains (**FF/FF**) or of mixed H/F chains (**HF/HF**, **HH/HF**) are colored in blue or hatched in grey/blue, respectively. Parameters are defined in Table 2.

Conclusion

The present study has considered two families of polycatenar materials, in which one or more hydrocarbon chains have been replaced by semiperfluorocarbon chains. The resulting behavior is dominated by two effects. Firstly, the fluorocarbon element of the chains occupies a greater volume than the hydrocarbon equivalent and this is seen most clearly for the tetracatenar compounds where this

increase in volume on replacing hydrocarbon by fluorocarbon has sufficient effect on the interfacial curvature to change from a lamellar (SmC) phase (**13**) into a Col_h phase (**FF/FF**, **HF/HF** and **HH/HF**). The lattice parameters for these columnar phases are all very similar showing that there are no other packing effects observed. Secondly, there is the mutual incompatibility between hydrocarbon and fluorocarbon chains, and how this is accommodated when the molecules contain both. For the tricatenar materials, the phase behavior with or without fluorocarbon chain is a SmC phase and the major difference observed is a doubling of the lamellar periodicity when a fluorocarbon chain is included as the system forms a bilayer, which keeps like chains with like. In the tetracatenar systems it is more subtle. Replacing one hydrocarbon chain in a 3-position with its semiperfluorocarbon analogue (**HH/HF**) tips the balance into Col_h from SmC phase and this is also true when a second semiperfluorocarbon chain is added into the 3'-position (**HF/HF**). As noted above, there is nothing remarkable about the lattice parameters in these Col_h phases and so these semiperfluorocarbon chains are evidently readily accommodated alongside their hydrocarbon equivalents. However, **HF/HF** and **HH/HF** do show a broad reflection (= loose correlation) corresponding to a 19 Å periodicity, which reveals the formation of regular 'islands' of fluorocarbon in the structure reflecting the amphiphilic nature of these materials. Replacing the remaining two hydrocarbon chains (**FF/FF**) also gives a compound with a Col_h phase but with no 19 Å periodicity as now there is only one type of terminal chain – semiperfluorocarbon. Compound **HH/FF** is isomeric with **HF/HF**, the difference being that the two semiperfluorocarbon chains in **HH/FF** are at one end of the molecule. Under these circumstances, the molecule shows a pronounced amphiphilicity so that the increase in chain volume destabilizes the SmC phase as expected. However, the need for like ends of the molecules to associate evidently precludes the formation of a phase with hexagonal symmetry and rather a phase of lower (rectangular) symmetry forms with large lattice parameters. One of the parameters is consistent with a lamellar bilayer, which suggests that the phase is ribbon-like and is also consistent with separation between the two chain types. It is important to note that the structural arguments used here are based on: (i) a previous and very solid understanding of the organization in the mesophases of polycatenar systems, (ii) the availability from numerous studies of volumetric data from studies using dilatometry and (iii) the availability of good-quality X-ray data analyzed in the light of (i) and (ii).

Supporting Information

The Supporting Information contains: details of the equipment and methods used; a description and details of the syntheses employed including analytical data; a description of the liquid crystal properties of the intermediate compounds (most of which are new); representative optical textures for all of the final products.

Acknowledgements

AG would like to acknowledge the Dinu Patriciu Foundation for sponsorship through the award of an 'Open Horizons' Excellence Studentship; MCT thanks the National Sun Yat-sen University for provision of a

scholarship, and BD and BH thank the CNRS and the Université de Strasbourg for support. The authors thank Rachel Bean for acquiring some images in Figure 2.

References:

1. Guittard, F.; Taffin de Givenchy, E.; Geribaldi, S.; Cambon, A. Highly Fluorinated Thermotropic Liquid Crystals: an Update. *J. Fluorine Chem.* **1999**, *100*, 85-96.
2. Kirsch, P. Fluorine in Liquid Crystal Design for Display Applications. *J. Fluorine Chem.* **2015**, *177*, 29-36.
3. Bremer, M.; Kirsch, P.; Klasen-Memmer, M.; Tarumi, K. The TV in Your Pocket: Development of Liquid-Crystal Materials for the New Millennium. *Angew. Chem., Int. Ed.*, **2013**, *52*, 8880–8896.
4. Tschierske, C. Fluorinated Liquid Crystals: Design of Soft Nanostructures and Increased Complexity of Self-Assembly by Perfluorinated Segments. *Top. Curr. Chem.* **2012**, *318*, 1–108.
5. Pauling, L. *The Nature of the Chemical Bond and the Structure of Molecules and Crystals: An Introduction to Modern Structural Chemistry*; Cornell University Press: Ithaca, NY, 1940.
6. O'Hagan, D. Understanding Organofluorine Chemistry. An Introduction to the C-F Bond. *Chem. Soc. Rev.* **2008**, *37*, 308-31.
7. Arehart, S. V.; Pugh, C. Induction of Smectic Layering in Nematic Liquid Crystals Using Immiscible Components. 1. Laterally Attached Side-Chain Liquid Crystalline Poly(norbornene)s and Their Low Molar Mass Analogs with Hydrocarbon/Fluorocarbon Substituents. *J. Am. Chem. Soc.* **1997**, *119*, 3027-3037.
8. Shreenivasa Murthi, H. N.; Sadashiva, B. K. Influence of a Fluorine Substituent on the Mesomorphic Properties of Unsymmetrical Five-ring Bent-core Compounds. *J. Mater. Chem.* **2004**, *14*, 2813-2821.
9. Reddy, R. A.; Sadashiva, B. K. Influence of Fluorine Substituent on the Mesomorphic Properties of Five-ring Ester Banana-shaped Molecules. *Liq. Cryst.* 2003, *30*, 1031-1050.
10. Eremin, A.; Wirth, I.; Diele, S.; Pelzl, G.; Schmalfuss, H.; Kresse, H.; Nadasi, H.; Fodor-Csorba, K.; Gacs-Baitz, E.; Weissflog, W. Structural Characterization of the New Polymorphic Mesophases Formed by Bent-core Molecules. *Liq. Cryst.* **2002**, *29*, 775-782.
11. Hird, M. Fluorinated Liquid Crystals – Properties and Applications. *Chem. Soc. Rev.* **2007**, *36*, 2070-2095.
12. Shen, D; Pegenau, A.; Diele, S.; Wirth, I.; Tschierske, C. Molecular Design of Nonchiral Bent-Core Liquid Crystals with Antiferroelectric Properties. *J. Am. Chem. Soc.* **2000**, *122,* 1593-1601.
13. Krafft, M. P.; Riess, J. G. Chemistry, Physical Chemistry, and Uses of Molecular Fluorocarbon-Hydrocarbon Diblocks, Triblocks, and Related Compounds - Unique "Apolar" Components for Self-Assembled Colloid and Interface Engineering. *Chem. Rev.* **2009**, *109,* 1714−1792.
14. Fleetwood, M. C.; McCoy, A. M.; Mecozzi, S. Synthesis and Characterization of Environmentally Benign, Semifluorinated Polymers and their Applications in Drug Delivery. *J. Fluorine Chem.* **2016**, *190*, 75-80.
15. Martin, O. M.; Yu, L.; Mecozzi, S. Solution Self-assembly and Solid State Properties of Fluorinated Amphiphilic Calix[4]arenes. *Chem. Comm.* **2005**, *39*, 4964-4966.
16. Gladysz, J. A.; Curran, D. P.; Horváth, I. T. *Handb. Fluorous Chem.*; WILEY-VCH Verlag GmbH: Weinheim, 2004.
17. Riess, J. G. Fluorous Micro- and Nanophases with a Biomedical Perspective. *Tetrahedron*, **2002**, *58*, 4113−4131.
18. Sadtler, V. M.; Giulieri, F.; Krafft, M. P.; Riess, J. G. Micellisation and Adsorption of Fluorinated Amphiphiles: Questioning the 1CF2 ≈ 1.5CH2 Rule. *Chem. Eur. J.*, **1998**, *4*, 1952−1956.
19. Percec, V.; Johansson, G.; Ungar, G.; Zhou, J. Fluorophobic Effect Induces the Self-Assembly of Semifluorinated Tapered Monodendrons Containing Crown Ethers into Supramolecular Columnar Dendrimers Which Exhibit a Homeotropic Hexagonal Columnar Liquid Crystalline Phase. *J. Am. Chem. Soc.* **1996**, *118*, 9855−9866.
20. Marczuk, P.; Lang, P.; Möller, M. Bulk Structure and Surface Activity of Semifluorinated Alkanes. *Colloids Surf., A* **2000**, *163*, 103−113.

21. Bondi, A. Van der Waals Volumes and Radii. *J. Phys. Chem.* **1964**, *68*, 441–451.
22. Somasundaran, P. *Encyclopedia of Surface and Colloid Science*; Taylor and Francis Group: Boca Raton, FL, 2006, vol. 4 (2nd ed.).
23. Edwin Law, C.-K.; Horváth, I. T. Synthesis and Applications of Fluorous Phosphines. *Org. Chem. Front.* **2016**, *3*, 1048-1062.
24. Atwood, D. A. *Sustainable Inorganic Chemistry*, Wiley, West Sussex, UK, **2016**.
25. Baker, R. T.; Tumas, W. Toward Greener Chemistry. *Science* **1999**, *284*, 1477-1479.
26. de Gracia Lux, C.; Donnio, B.; Heinrich, B.; Krafft, M. P. Thermal Behavior and High- and Low-Temperature Phase Structures of Gemini Fluorocarbon/Hydrocarbon Diblocks. *Langmuir* **2013**, *29*, 5325−5336.
27. Bury, I.; Heinrich, B.; Bourgogne, C.; Mehl, G. H.; Guillon D.; Donnio, B. Self-assembly and Liquid-crystalline Supramolecular Organisations of Semifluorinated Block Co-dendritic Molecules. *New J. Chem.* **2012**, *36*, 452–468.
28. Date, R. W.; Iglesias, E. F.; Rowe, K. E.; Elliott J. M.; Bruce, D. W. Metallomesogens by Ligand Design. *Dalton Trans.* **2003**, *1916*, 1914–1931.
29. Höpken, J.; Möller, M. On the Morphology of (Perfluoroalkyl)alkanes. *Macromolecules* **1992**, *25*, 2482-2489.
30. Viney, C.; Russell, T. P.; Deprero, L. E.; Twieg, R. J. Transitions to Liquid Crystalline Phases in a Semifluorinated Alkane. *Mol. Cryst. Liq. Cryst*. **1989**, *168*, 63-82.
31. Viney, C.; Twieg, R. J.; Russell, T. P.; Deprero, L. E. The Structural Basis of Transitions Between Highly Ordered Smectic Phases in Semifluorinated Alkanes. *Liq. Cryst*. **1989**, *5*, 1783-1788.
32. Pelzl, G.; Diele, S.; Lose, D.; Ostrovski, B.I.; Weissflog, W. The Influence of the Shape and the Incompatibility of Molecular Moieties on the Structure of Smectic Mesophases. *Cryst. Res. Technol.* **1997**, *32*, 99-109;
33. Lose, D.; Diele, S.; Pelzl, G.; Dietzmann, E.; Weissflog, W. Frustrated smectic phases in swallow-tailed compounds with perfluorinated chains. *Liq. Cryst.*, **1998**, *24*, 707-717.
34. Pegenau, A.; Cheng, X. H.; Tschierske, C.; Göring, P.; Diele, S. Formation of Mesophases Based on Micro-segregation: Columnar Liquid-crystalline Phases of First Generation Dendrimers with Perfluorinated Segments. *New J. Chem.* **1999**, *23*, 465-467.
35. Cheng, X. H.; Das, M. K.; Diele, S.; Tschierske, C. Influence of Semiperfluorinated Chains on the Liquid Crystalline Properties of Amphiphilic Polyols: Novel Materials with Thermotropic Lamellar, Columnar, Bicontinuous Cubic, and Micellar Cubic Mesophases. *Langmuir* **2002**, *18,* 6521-6529.
36. Cheng, X. H.; Diele, S.; Tschierske, C. Molecular Design of Liquid-crystalline Block Molecules : Semifluorinated Pentaerythritol Tetrabenzoates Exhibiting Lamellar, Columnar and Cubic Mesophases, *Angew. Chem. Int. Ed.* **2000**, *39,* 592-595.
37. Kohlmeier, A.; Janietz, D. Hydrogen-bonded Block Mesogens Derived from Semiperfluorinated Benzoic Acids and the Non-mesogenic 1,2-bis(4-pyridyl)ethylene. *Liq. Cryst.*, **2007**, *34*, 65–71.
38. Malthête, J.; Nguyen, H. T.; Destrade, C. Phasmids and Polycatenar Mesogens. *Liq. Cryst.* **1993**, *13*, 171–187.
39. Nguyen, H. T.; Destrade, C.; Malthête, J. Phasmids and Polycatenar Mesogens. *Adv. Mater.* **1997**, *9*, 375–388.
40. Fazio, D.; Mongin, C.; Donnio, B.; Galerne, Y.; Guillon, D.; Bruce, D. W. Bending and Shaping: Cubics, Calamitics and Columnars. *J. Mater. Chem.* **2001**, *11*, 2852–2863.
41. Guillon, D.; Heinrich, B.; Ribeiro, A. C.; Cruz, C.; Nguyen, H.T. Thermotropic Lamellar-to-Columnar Phase Transition Exhibited by a Biforked Compound, *Mol. Cryst. Liq. Cryst.* **1998**, *317*, 51-64.
42. Donnio, B.; Bruce, D. W. Liquid-crystalline Complexes of Palladium(II) and Platinum(II) with Di- and Tri-alkoxystilbazoles: Ligand Control of Mesomorphism. *J. Chem. Soc*., *Dalton Trans*., **1997**, 2745–2755.
43. Donnio, B.; Heinrich, B.; Allouchi, H.; Kain, J.; Diele, S.; Guillon, D.; Bruce, D. W. A Generalized Model for the Molecular Arrangement in the Columnar Mesophases of Polycatenar Mesogens. Crystal and Molecular Structure of Two Hexacatenar Mesogens. *J. Am. Chem. Soc.* **2004**, *126*, 15258-15268.

44. Smirnova, A. I.; Heinrich, B.; Donnio, B.; Bruce, D. W. The Influence of Lateral Fluorination and Cyanation on the Mesomorphism of Polycatenar Mesogens and the Nature of the SmC Phase therein. *RSC Adv.* **2015**, *5*, 75149-75159.
45. Alvey, L. J.; Meier, R.; Soos, T.; Bernatis, P.; Gladysz, J. A. Syntheses and Carbonyliridium Complexes of Unsymmetrically Substituted Fluorous Trialkylphosphanes: Precision Tuning of Electronic Properties, Including Insulation of the Perfluoralkyl Groups. *Eur. J. Inorg. Chem.* **2000**, *9*, 1975-1983.
46. Johansson, G.; Percec, V., Ungar, G.; Zhou, J. Fluorophobic Effect in the Self-Assembly of Polymers and Model Compounds Containing Tapered Groups into Supramolecular Columns. *Macromolecules* **1996**, *29*, 646–660.
47. Luscombe, C. K.; Proemmel, S.; Huck, W. T. S.; Holmes, A. B.; Fukushima, H. Synthesis of Supercritical Carbon Dioxide Soluble Perfluorinated Dendrons for Surface Modification. *J. Org. Chem*. **2007**, *72*, 5505-5513.
48. Percec, V.; Glodde, M.; Peterca, M.; Rapp, A.; Schnell, I.; Spiess, H. W.; Bera, T. K.; Miura, Y.; Balagurusamy, V. S. K.; Aqad, E.; Heiney, P. A. Self-assembly of Semifluorinated Dendrons Attached to Electron-Donor Groups Mediates Their π-Stacking via a Helical Pyramidal Column. *Chem. - Eur. J.* **2006**, *12*, 6298-6314.
49. Smirnova, A. I.; Zharnikova, N. V.; Donnio, B.; Bruce, D. W. The Influence of Lateral Apolar Substituents on the Mesomorphic Behaviour of Tetracatenar Liquid Crystals. *Russ. J. Gen. Chem.*, 2010, **80**, 1331-1340.
50. Marcos, M.; Giménez, R.; Serrano, J. L.; Donnio, B.; Heinrich, B.; Guillon, D. Dendromesogens: Liquid Crystal Organisations of Poly(amidoamine) Dendrimers versus Starburst Structures, *Chem. Eur. J.* **2001**, *7*, 1006-1013.
51. Myśliwiec, D.; Donnio, B.; Chmielewski, P. J.; Heinrich, B.; Stępień, M. Peripherally Fused Porphyrins via the Scholl Reaction: Synthesis, Self-Assembly, and Mesomorphism. *J. Am. Chem. Soc.* **2012**, *134*, 4822-4833.
52. Alameddine, B.; Aebischer, O. F.; Heinrich, B.; Guillon, D.; Donnio, B.; Jenny, T. A. Influence of Linear and Branched Perfluoroalkylated Side Chains on the π-π Stacking Behaviour of Hexa-peri-hexabenzocoronene and Thermotropic Properties. *Supramolecular Chem.* **2014**, *26*, 125-137.
53. Tschierske, C. Liquid Crystal Engineering – New Complex Mesophase Structures and their Relations to Polymer Morphologies, Nanoscale Patterning and Crystal Engineering. *Chem. Soc. Rev.* **2007**, *36*, 1930-1970.
54. Nishikawa, E.; Yamamoto, J.; Yokoyama, H. Nano-segregated Structures of Hydrogen-bonded Mesogens with Perfluorinated Moieities: Cubic Phase Formation and First Order Smectic A to Smectic C Phase Transition. *Liq. Cryst.* **2003**, *30*, 785-798.
55. Nishikawa, E.; Yamamoto, J.; Yokoyama, H. *J. Mater. Chem.* **2003**, *13*, 1887-1893.
56. Allouchi, H.; Cotrait, M.; Guillon, D.;Heinrich, B.; Nguyen, H. T. Relationships between the Crystalline and the Smectic C Structures of a Biforked Mesogen. *Chem. Mater*. **1995**, *7*, 2252-2258.
57. Nguyen, H. T.; Destrade, C.; Levelut, A. M.; Malthête, J. Biforked Mesogens: a New Type of Thermotropic Liquid Crystals. *J. Phys.* **1986**, *47*, 553-557.
58. Pitto-Barry, A.; Barry, N. P. E.; Russo, V.; Heinrich, B.; Donnio, B.; Therrien, B.; Deschenaux, R. Designing Supramolecular Liquid-Crystalline Hybrids from Pyrenyl-containing Dendrimers and Arene Ruthenium Metallacycles. *J. Am. Chem. Soc.* **2014**, *136*, 17616-17625.
59. Ribeiro, A. C.; Heinrich, B.; Cruz, C.; Nguyen, H. T.; Diele, S.; Schröder, M. W.; Guillon, D. Rectangular to Hexagonal Columnar Phase Transition Exhibited by a Biforked Mesogen. *Eur. Phys. J. E* **2003**, *10*, 143-151.
60. Nguyen, H. T.; Destrade, C.; Allouchi, H.; Bideau, J. P.; Cotrait, M.; Guillon, D.; Weber, P.; Malthete, J. Phasmid and Biforked Mesogens with Thiobenzoate End Groups. *Liq. Cryst.* **1993**, *15*, 435-449.

TOC Graphic

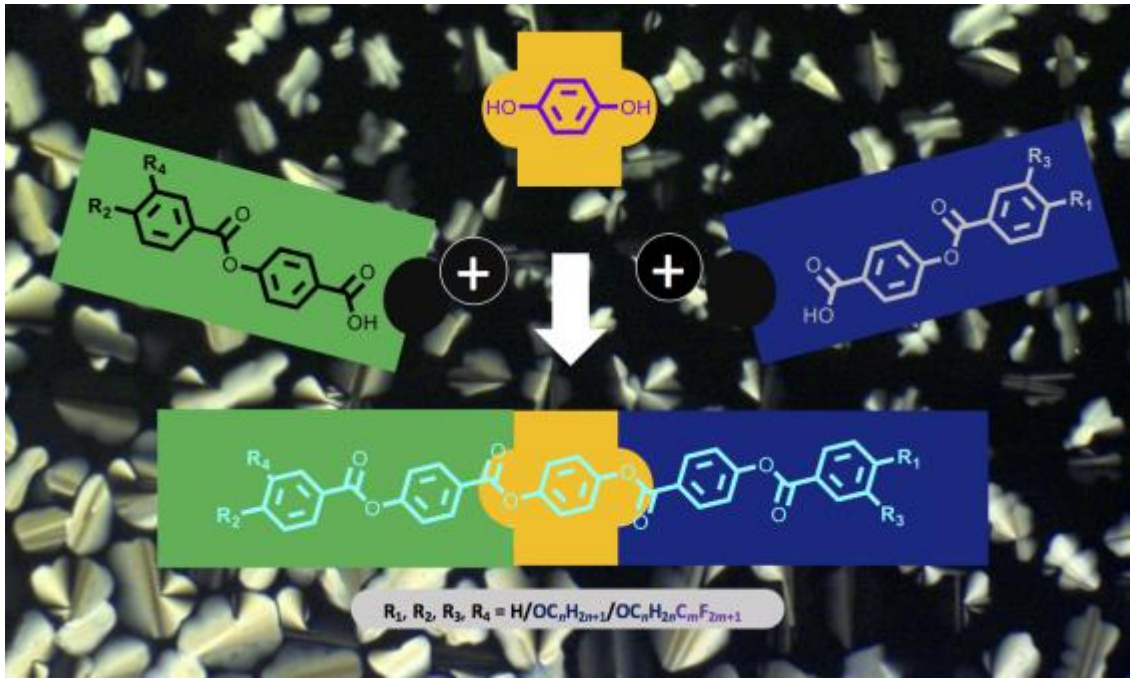
HO
OH
R4
R2
O
O
O
OH
+
+
R3
R1
O
O
HO
R4
R2
R1
R3
R1, R2, R3, R4 = H/OCnH2n+1/OCnH2nCmF2m+1